

EDITORS

Thomas M. Moses and
Shane F. McClure
GIA Laboratory

APATITE in SPESSARTINE

The science of gemology is a continuous and unlimited path of learning, with many side trails and stops along the way. One of the trails we like to explore are new inclusion-to-host relationships, because this information and the means used to gather it increase our knowledge and make us more effective laboratory gemologists.

Just such an opportunity arose when the Carlsbad lab was asked to identify a small group of assorted Sri Lankan gems. One of these gems was a bright orange 1.84 ct round mixed cut (figure 1) that proved to be spessartine. The garnet's refractive index was just below the limits of the refractometer at 1.80, and its visible spectrum showed strong manganese absorption. The presence of several dark blue-green rounded birefringent crystals (figure 2) sparked our curiosity, because we had never before encountered similar inclusions in a spessartine. Another interesting feature of these inclusions was that they, in turn, appeared to contain solid inclusions of their own.



Figure 1. Discovered in a group of Sri Lankan gems, this 1.84 ct bright orange spessartine contains very interesting dark blue-green inclusions.

We speculated that the blue-green inclusions might be apatite, since apatite crystals of similar color and condition have been observed in spinel and sapphire from Sri Lanka. This form of pre-analysis speculation is a way to stimulate thought and not allow the analytical apparatus to think for you. Since one of the inclusions had been polished through on the crown and exposed to the surface of the host garnet, it made an ideal target for Raman testing. The Raman spectra confirmed our suspicion, and as a bonus enabled us to identify an inclusion in the apatite as a carbonate, possibly calcite. We are not aware of any previous reports of such inclusions in spessartine from any

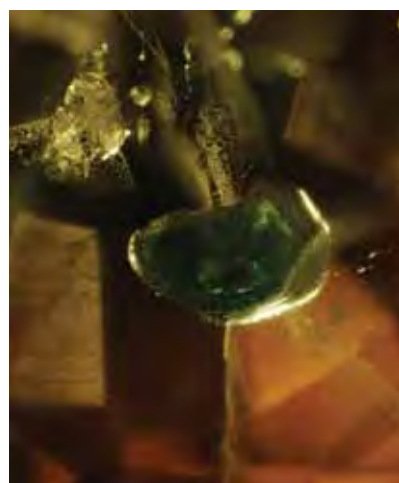


Figure 2. Raman analysis proved that the blue-green inclusions were apatite, while the solids within the apatite crystals were identified as a carbonate. The apatite inclusion pictured here is 0.91 mm in longest dimension.

locality, and thus believe this is a first observation.

John I. Koivula and Alethea Inns

DIAMOND

Atypical Photoluminescence Feature in a Colorless Type IIa

Type IIa diamonds typically contain almost no impurity-related defects. Any color present in most type IIa

Editors' note: All items are written by staff members of the GIA Laboratory.

GEMS & GEMOLOGY, Vol. 43, No. 4, pp. 358–365.
© 2007 Gemological Institute of America

stones is usually ascribed to extended defects, such as slip planes due to plastic deformation. While nitrogen is present in many type IIa diamonds, it is at such a low concentration that it is not detectable by mid-infrared spectroscopy. Often, however, nitrogen-related features (such as N-V centers and the H3 and H4 centers) are clearly resolved with photoluminescence (PL) spectroscopy, which shows that nitrogen is indeed present, even in aggregated forms.

Recently during routine testing of a 1.01 ct, E-color, pear-shaped type IIa diamond (figure 3) in the New York laboratory, we discovered the presence of a defect previously believed to occur only in certain type I diamonds. This defect is responsible for the so-called “480 nm band,” which is typically seen in the absorption spectra of highly saturated orangy yellow to yellowish orange type I stones that also display medium-to-strong yellow fluorescence (see, e.g., Spring 2007 Lab Notes, pp. 49–50). Generally, these stones are a mixture of low- to medium-nitrogen type IaA and type Ib material; that is, the nitrogen is present as isolated single atoms and nearest-neighbor pairs (A. T. Collins et al., “Optical studies of vibronic bands in yellow luminescing diamonds,” *Journal of Physics C*, Vol. 15, 1982, pp. 147–158). This feature is also found in the absorption spectra of chameleon diamonds. The exact structure and makeup of the 480 nm band defect is not known, but it has been suggested that it may be a complex defect containing nitrogen, hydrogen, and/or nickel (A. T. Collins, “Colour centres in diamond,” *Journal of Gemmology*, Vol. 18, 1982, pp. 37–75).

The 480 nm band was not detected with absorption spectroscopy, since this stone was near colorless. The PL spectrum of the diamond at 488 nm excitation showed the distinct structure of the 480 nm band in luminescence, centered at ~700 nm (figure 4). The numerous phonon replicas visible between 600 and 700 nm indicate that this defect is strongly coupled to lattice vibrations. As expected, no zero-phonon line was detected for this sys-

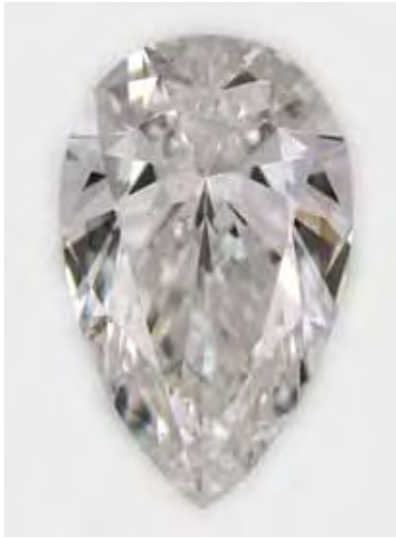


Figure 3. This 1.01 ct pear-shaped type IIa diamond shows photoluminescence due to the 480 nm band defect, which was previously thought to occur only in type I diamonds.

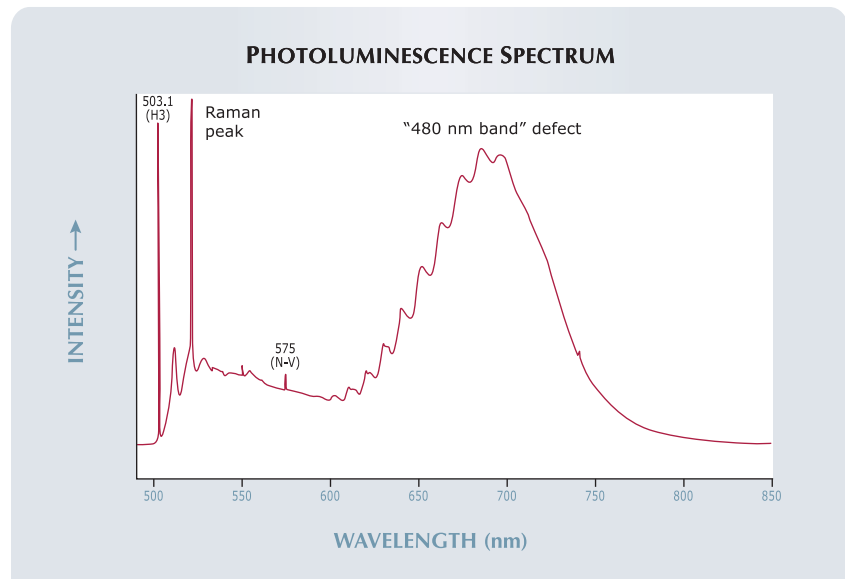
tem in luminescence. Note also that strong emission from the H3 defect at 503.1 nm was present in this spec-

trum. Multiple measurements at various locations around the stone showed that the 480 nm band defect was not homogeneously distributed.

Visual examination of the diamond while it was exposed to long-wave UV radiation revealed a faint patch of orangy yellow fluorescence centered around a crystal inclusion; unfortunately, this inclusion was too deep within the stone to be identified by Raman analysis. PL spectra taken at 830 nm excitation at the same varied locations showed sharp doublet peaks at 883/884 nm (i.e., the 1.40 eV center), which are known to be related to a substitutional nickel impurity (figure 5, W. Wang et al., “Natural type Ia diamond with green-yellow color due to Ni-related defects,” *Fall 2007 Gems & Gemology*, pp. 240–243).

Because the 480 nm band has previously been detected only in type I stones, we have theorized that the defect is likely nitrogen-related. The present findings do not disprove this speculation, since nitrogen is known to be present in type II material, although at very low concentrations.

Figure 4. The photoluminescence spectrum at 488 nm excitation shows the broad luminescence feature due to the 480 nm band defect, centered at about 700 nm. Also present are the H3 defect at 503.1 nm and its side-band, and a sharp peak at 575 nm due to the N-V center.



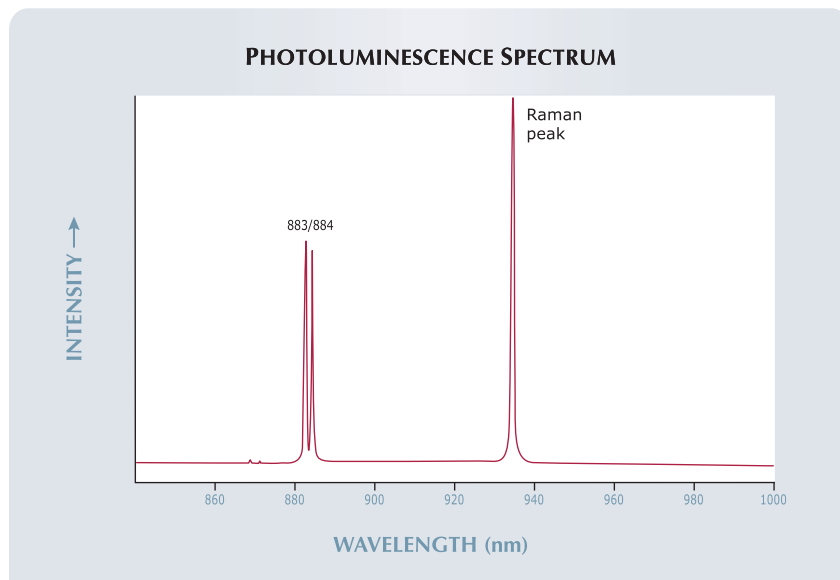


Figure 5. The photoluminescence spectrum at 830 nm excitation shows a doublet at 883/884 nm due to substitutional nickel.

Rather, this example may indicate that the correlation between the 480 nm band and the presence of nitrogen is not very strong, or that the 480 nm band defect is related to nickel.

Jon Neal

Inclusions Fit for a Holiday Season

Mineral inclusions are very useful when identifying diamond, as well as in determining its origin of color and basic geology. Often, they are also the determining factor in setting the clarity grade. Unusual inclusion arrangements can be a pleasure to observe and can enhance interest in the stone when the internal feature resembles a heart or other familiar object. However, diamonds with euhedral crystals displaying vibrant color are exceedingly rare.

Recently, a grader in the New York lab observed just such features in a 1.01 ct, F-color, round brilliant diamond (figure 6) with well-formed bluish green and reddish orange crystal inclusions. In light of the upcoming holiday season, the grader fondly referred to the find as the “Christmas stone” due to its combination of col-

ors. Although we have documented such eclogitic inclusions before (see, e.g., Spring 2002 Lab Notes, pp. 80–81; W. Wang et al., “Natural type Ia dia-

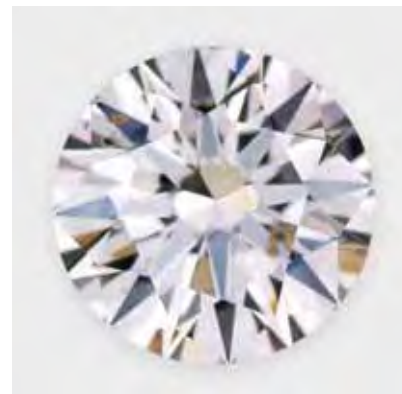


Figure 6. This 1.01 ct diamond is distinguished by the presence of a reddish orange garnet crystal and bluish green omphacite crystals, visible at approximately the 10 o'clock position.

mond with green-yellow color due to Ni-related defects,” Fall 2007 *Gems & Gemology*, pp. 240–243), this inclusion scene was unusual because of the proximity of the crystals to each other and the vibrancy of their colors (figure 7). Also interesting was the discovery

Figure 7. With magnification, the vibrant colors of the garnet and omphacite crystals become more apparent. Note that the crystals are set apart by stress cracks. Magnified 100×.



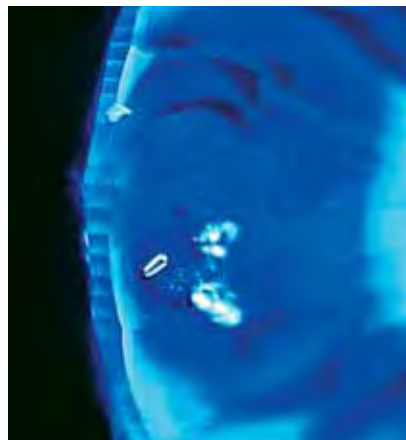


Figure 8. This DiamondView image shows that the crystals in figure 7 were trapped with a second omphacite crystal within a single octahedral growth sector.

that both crystals had formed within the same growth sector, as can be seen from the DiamondView image in figure 8, which distinctly illustrates the inclusions. Using Raman analysis (830 nm laser), we identified the reddish orange crystal as almandine-rich garnet and the bluish green crystal as omphacite (a pyroxene).

These inclusions are an excellent example of well-formed syngenetic crystals (i.e., formed at the same time as the host) in diamond. In this case, they were also the features that led to an SI₂ clarity grade, a perhaps disappointing result given the diamond's unique beauty and character. GIA diamond graders view thousands of stones annually, and it is refreshing to see a grouping of inclusions that readily tell a story of the diamond's distinctive growth.

Bonny S. Alphonso, Jennifer Schan, and Paul Johnson

With Large Etch Channels Filled with Iron Sulfides

Etch channels have been found in both type I and II diamonds from almost every locality (see T. Lu et al., "Observation of etch channels in sev-

eral natural diamonds," *Diamond and Related Materials*, Vol. 10, 2001, pp. 68–75). They occur in a variety of shapes, from nearly straight lines to irregular worm-like or branching patterns (see, e.g., Summer 2006 Lab Notes, p. 165). The New York laboratory recently encountered an interesting example of this feature, a 0.57 ct Fancy Deep brownish yellow round brilliant that had eye-visible etch channels with multiple branches that contained a dark brown material (figure 9).

Examination with a gemological microscope revealed intense brown radiation stains on the outer walls of the etch channels that locally penetrated into the adjacent diamond a short distance. Most of the channels had hexagonal openings (from 0.2 × 0.1 mm to 0.55 × 0.6 mm in diameter) at and just under the girdle (see figure 10). The main channel was partially polished out, so it was exposed from the girdle across the crown facets to the table, where it broke the surface of the table facet (again, see figure 10). Large cavities in this channel were possibly caused by the polishing process. The large opening in the table contained a transparent material that was completely surrounded by the dark brown material. Multiple chan-

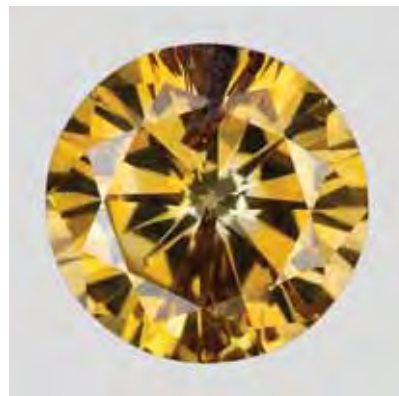
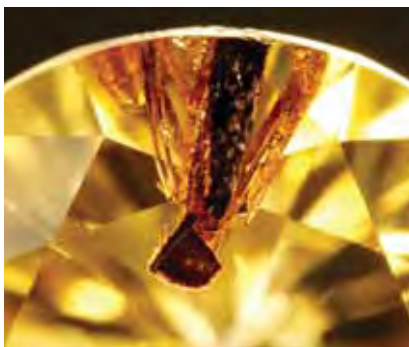


Figure 9. This 0.57 ct Fancy Deep brownish yellow diamond has several etch channels, which appear to contain a dark brown material.

nels branched out from this main channel, with a few isolated channels elsewhere in the diamond.

DiamondView images showed green-fluorescing growth zones, while the materials in the etch channels fluoresced blue (figure 11). As can be seen in figure 11, the etch channels intersected different growth zones, which suggests they were formed epigenetically, after the diamond had completed its growth. Raman spectroscopy

Figure 10. Multiple etch channels in the 0.57 ct diamond branch from the main channel, which breaks the surface of the table facet (0.55 × 0.6 mm; left). At this opening, it can be seen that the channel contains a transparent material that is completely surrounded by a dark brown material, which is responsible for the perceived color. Part of the main channel was also exposed on the crown facets, and cavities can be seen on its surface. The etch channels show roughly hexagonal outlines where they reach the pavilion surface (right).



identified the dark brown material as predominantly pyrrhotite, a common iron sulfide inclusion in diamonds. At a few spots inside the pyrrhotite, pentlandite (a Ni-rich iron sulfide) was also identified. Raman spectroscopy identified the transparent material in the large opening in the table as diamond.

Filled etch channels have been reported previously; they may contain iron hydroxides, black host-rock materials, or serpentine (see, e.g., R. M. Davies et al., "Inclusions in diamonds from the K14 and K10 kimberlites, Buffalo Hills, Alberta, Canada: Diamond growth in a plume?" *Lithos*, Vol. 77, 2004, pp. 99–111). The unusual presence of pyrrhotite and pentlandite in these etch channels suggests that iron sulfide inclusions can be formed epigenetically, as well as syngenetically, in diamonds. It further suggests that Fe-Ni monosulfide solutions can be injected into a diamond even after post-growth etching.

Kyaw Soe Moe, Surjit Dillon, and Thomas Gelb

Figure 11. In this DiamondView image, the etch channels intersect different growth zones showing different intensities of green, while the dark brown material fluoresces blue. This image further suggests that the etch channels were created and the filling material (pyrrhotite and pentlandite) was deposited after the diamond was fully formed.

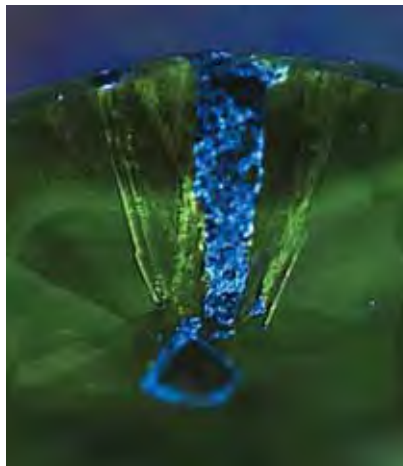


Figure 12. The 3.06 ct natural black diamond on the left, when viewed with strong transmitted light (right), shows an unusually long, straight etch channel as well as dark clouds of inclusions.

Natural Black DIAMOND with Oriented Etch Channel

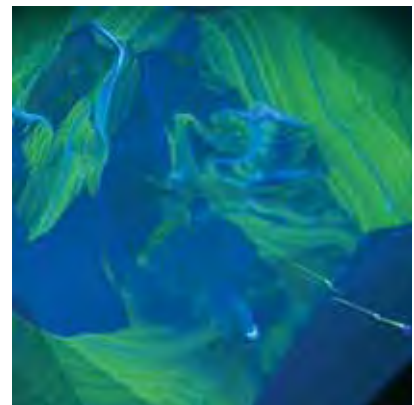
Most "black" diamonds currently on the market are treated color, created either by heating or by exposure to intense radiation. Natural black diamonds suitable for jewelry use are not common. Recently, however, the New York laboratory examined an interesting natural-color black diamond that also had a well-developed and oriented etch channel.

This 3.06 ct diamond (figure 12) was color graded Fancy black. Infrared spectroscopy showed that it was type Ia with a relatively high concentration of hydrogen. The UV-Vis spectrum did not display any resolvable peaks due to the near-opacity of the stone. Energy-dispersive X-ray fluorescence (EDXRF) analysis indicated the presence of Fe and Ni, which have also been observed in black diamonds from Siberia (S. V. Titkov et al., "An investigation into the cause of color in natural black diamonds from Siberia," Fall 2003 *Gems & Gemology*, pp. 200–209). Infrared and photoluminescence spectroscopy did not reveal any evidence of treatment; the black color was undoubtedly caused by the presence of dark sectorial clouds that absorbed virtually all light.

The diamond's most notable feature was a well-developed etch chan-

nel that traversed almost half the stone from under the center of the table to one of the crown facets (figure 12, right), where it reached the surface with an approximately 10 μm wide near oval-shaped opening. Diamond-View fluorescence imaging showed that the growth sectors were well aligned with respect to crystallographic symmetry and that the dark clouds generally correlated with the growth

Figure 13. The DiamondView fluorescence image of the stone in figure 12 reveals that the dark clouds correlate with cubic growth sectors and that the etch channel (visible in the lower right) is crystallographically aligned.



pattern (figure 13). It further indicated that the etch channel was perfectly aligned along the [111] direction. An additional frosty etch mark was present at one of the corners of the stone (again, see figure 12), but no other etch features were observed.

Not only does the testing of this stone prove that it is a natural-color black diamond, but the fluorescence imaging also confirms that etch-channel development follows growth zones and localized lattice defects, consistent with the earlier report by A. Nemirovskaya and W. Wang ("Diamond with unusual etch channel," Summer 2006 Lab Notes, p. 165).

Ren Lu and Wuyi Wang

The Pareidolia of Diamonds

Have you ever gazed up at the sky on a warm spring day and seen a human face in the clouds? Or a horse? Or another fanciful image? Now examine figure 14. What do you see? Some might see a feather with a crystal above it; others might see a person tossing a ball. *Pareidolia* is the term that psychologists use to describe the phenomenon in which the brain qualitatively assigns familiar shapes to random, abstract forms.

In seeming contrast, cutting dia-

Figure 14. This diamond inclusion scene, composed of a feather and a crystal, reminds some observers of a person tossing a ball.



Figure 15. This unusual diamond (approximately 12.0 × 6.7 × 3.5 mm) has been faceted in the shape of a fish.

monds is nominally a more quantitative process in which the manufacturer calculates the most profitable combination of clarity, cut, and weight retention. This, of course, is based on sober judgments regarding specific shapes with corresponding angles and proportions that result in an attractive diamond. That being said, there are exceptions to every rule, and not all diamonds are so straightforward in the decision process. Often creativity is needed to determine what shape will result in sufficient weight retention, good clarity, and an attractive appearance. And pareidolia may help that creativity. This is especially important in cases of oddly propor-

tioned or otherwise "difficult" rough, which can be fashioned into truly fanciful shapes such as that in figure 15, which shows a 1.80 ct diamond cut in the shape of a fish.

Coincidentally, the New York laboratory recently encountered the oddly shaped 13.25 ct crystal in figure 16. Microscopic examination showed a number of graphitized inclusions and small crystals. The diamond was type IaB>A, as determined by infrared spectroscopy, and showed strong blue fluorescence to long-wave UV radiation and moderate yellow fluorescence to short-wave UV. While examining this crystal, several of the lab's graders

Figure 16. This large rough diamond (25.68 × 6.26 × 7.60 mm) also reminded some graders of a fish.



referred to it as “the fish” due to their perception of its shape. Those of us who had also seen the faceted fish felt they had an uncanny resemblance. This pareidolic perception is distinctive to each individual, so if the cutter also visualized this rough as a fish, perhaps he would create a finished stone similar to figure 15.

Joshua Sheby and Jason Darley

A Notable EMERALD Carving

Emerald has long been a popular carving material, and it is not unusual for carved emerald beads, tablets, and the like to be submitted to gemological laboratories such as GIA (see, e.g., Lab Notes—Fall 1981, pp. 161–162, and Winter 1994, pp. 264–265; Gem News International—Summer 2001, p. 145, and Fall 2002, pp. 262–263). It is unusual, however, to see an emerald carving the size of the 2,620.70 ct statue that Jeffery Bergman of Primagem submitted to the Bangkok laboratory for identification in November 2007 (figure 17).

The carving was of a standing Buddha, or *Baang Haarm Yaard* in Thai. It is said that the standing posture represents the Buddha’s admonition to his family members to stop quarreling among themselves. This is also the Buddha image for those born on a Monday.

The size and shape of the medium-to-dark green statue made standard gemological testing difficult, so we used Raman spectroscopy to obtain a positive identification of the material as beryl. Microscopic examination revealed rectangular colorless crystals, brown crystals, two-phase inclusions, and partially healed fractures, proving the emerald was of natural origin. It also confirmed that the carving was fashioned from a single crystal.

Due to their growth conditions in nature and the recovery methods used by miners, most emeralds contain fractures. For this reason, it is common to apply oil to improve their apparent clarity, and such was the case with this Buddha. In fact, when we opened the plastic bag holding the item, the smell of cedarwood oil was



Figure 17. This standing Buddha (15.70 × 6.50 × 5.30 cm) was carved from a single emerald crystal.

obvious. Examination with a gemological microscope revealed a viscous liquid in fine crevices of the carving, providing clear evidence of oiling. Because the image was predominantly translucent to opaque with very few transparent areas, the normal clarity enhancement criteria used for GIA Emerald Reports was not applied to this piece.

The size and shape of the carving, as well as its having been fashioned from a single crystal, made this standing Buddha statue noteworthy.

Garry Du Toit

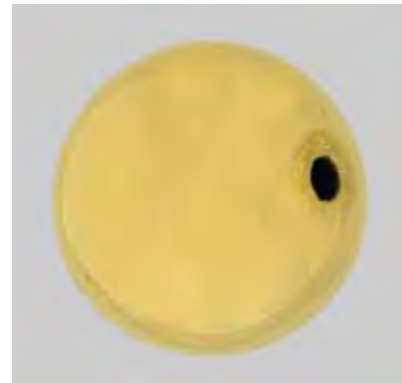
Gold Coated ONYX

Recently, a client submitted the 10.45 mm (7.45 ct) round yellow metal bead in figure 18 to the Carlsbad laboratory for identification. While the lab makes every effort to avoid destructive methods in gemological testing, this client permitted us to polish a flat on the surface of the bead in order to study the material underneath (fig-



ure 19). The polished flat had RI values of 1.540–1.547, a granular structure, and a Fourier-transform infrared signal corresponding to chalcedony. Qualitative chemical analysis (by EDXRF spectroscopy) of the coating revealed that it was mainly gold with trace amounts of other elements. As a

Figure 18. This 10.45 mm yellow metal bead proved to be gold-coated black onyx.



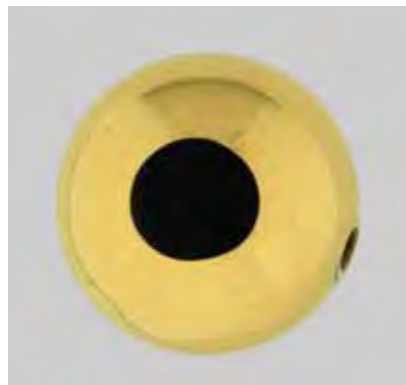


Figure 19. After the client allowed a flat to be polished on the bead, the black material underneath the gold was readily identified.

result, we issued a report stating “chalcedony, known in the trade as ‘Black Onyx,’ with a metallic coating composed primarily of gold.”

Over the years, the lab has received a few metal-coated articles for identification. Typically, this kind of material is extremely difficult, if not impossible, to identify using standard gemological methods.

Alethea Inns

SAPPHIRE with a Double Star

Recently, the New York laboratory received an unusual item for identification: a 3.78 ct light gray-blue oval sapphire cabochon showing not one but two separate well-formed stars when viewed under a single spot light (figure 20). Although we have seen corundum with superimposed double stars before (e.g., Fall 1993 Lab Notes, p. 212; Fall 1998 Lab Notes, p. 217), this is the first time we have documented two “side-by-side” stars in a single fashioned stone. In the previous cases, the overlapping stars were caused by lamellar twinning, with the rutile silk arranged in slightly different orientations from one layer to another.

In this cabochon, however, we noted that the two asteriated regions were separated by an irregular junc-

tion. Because of this irregularity, we concluded that the two silky areas were separate crystals with different orientations (i.e., they were not crystallographically related). The dual asterism was caused by the combination of the cabochon’s curvature and the slightly different orientation of the two sectors.

In addition to a rich concentration of pristine epitaxial silk and arrowhead twins following partial hexagonal growth, unaltered “fingerprint” inclusions supported the conclusion that the stone had not been heat treated. Although the two differently oriented regions kept the two stars separate, the arms were well-formed, well centered, and sharp. This “double” cab was truly a beautiful variation on one of nature’s more elegant phenomena.

David M. Kondo

Impregnated Glass Imitation of TURQUOISE

Turquoise is commonly treated by impregnation with either wax or a polymer, such as oil, to improve durability and luster. The Carlsbad laboratory frequently receives impregnated turquoise for testing, as well as numer-

Figure 20. This unusual double-star sapphire cabochon (10.75 × 7.00 × 4.20 mm) was likely fashioned from two intergrown crystals.

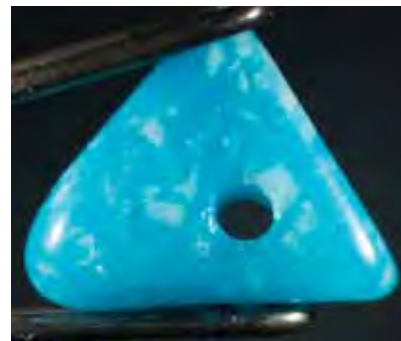


Figure 21. This 0.81 ct glass bead imitating turquoise also showed the presence of an oil filler.

ous dyed and/or impregnated turquoise imitations such as magnesite, howlite, and variscite, among others.

Recently, the lab received the 0.81 ct triangular blue bead in figure 21 for identification. The sample was transparent to semitransparent, and magnification revealed spherical and elongated gas bubbles, flow lines, and wave-like bands, and whitish granular crystal aggregates. The RI was 1.49 and the SG was 2.18, both of which are consistent for glass. Glass imitations (of all gem materials) are common. In this sample, however, the included crystals unexpectedly “sweated” when a thermal reaction tester was applied. FTIR spectroscopy revealed the presence of oil and typical glass peaks.

This is the first time we have come across a glass imitation for turquoise that also showed evidence of impregnation.

Alethea S. Inns

PHOTO CREDITS

Robert Weldon—1; John I. Koivula—2; Jian Xin (Jae) Liao—3, 6, 9, and 16; Jason Darley—7; Paul Johnson—8; Kyaw Soe Moe—10 and 11; Ren Lu—12 and 13; G. Robert Crowningshield—14; Unknown—15; Suchada Kittayachai-wattana—17; Robison McMurtry—18 and 19; Elizabeth Schrader—20; Alethea Inns—21.